



# Integration of Solar Energy in Grid-Connected EV Fast Charging Systems with UWBG Power Devices for Efficient and Sustainable Energy Management

Dr. J. Srinu Naick | M.C.V Suresh | B. Namitha | S.Bhargava Reddy | T. Srikanth | A.Pramodh Kumar

Department of Electrical and Electronics Engineering, Chadalawada Ramanamma Engineering College, Andhra Pradesh, India.

## To Cite this Article

Dr. J. Srinu Naick, M.C.V Suresh, B. Namitha, S.Bhargava Reddy, T. Srikanth & A.Pramodh Kumar (2025). Integration of Solar Energy in Grid-Connected EV Fast Charging Systems with UWBG Power Devices for Efficient and Sustainable Energy Management. International Journal for Modern Trends in Science and Technology, 11(09), 165-173. <https://doi.org/10.5281/zenodo.18124593>

## Article Info

Received: 02 September 2025; Accepted: 28 September 2025.; Published: 30 September 2025.

**Copyright** © The Authors ; This is an open access article distributed under the [Creative Commons Attribution License](#), which permits unrestricted use, distribution, and reproduction in any medium, provided the original work is properly cited.

KEYWORDS	ABSTRACT
Electric Vehicle Charging, Solar Integration, Grid-Tied Converter, Dual Active Bridge, Power Continuity, Renewable Energy, Hybrid Charging System, Gallium Oxide Comparison, Sustainable Infrastructure.	<p><i>The need to charge electric vehicles (EVs) quickly, reliably and at high power has created the need for quick and powerful charging systems. Most current systems use grid-connected off-board charging stations which are built with the help of advanced Gallium III Oxide (<math>Ga_2O_3</math>)-based ultra-wide bandgap (UWBG) power electronic components to provide high efficiency, rapid charging and high power density. Current systems have successfully provided rapid charging by utilizing the combination of bidirectional AC-DC converters and isolated DC-DC full bridge converters, however, all of these systems are dependent upon the grid. Therefore, these systems lack resiliency during power outages and limit the ability to integrate renewable energy sources into the system. In order to meet this void, the proposed system is introducing a new hybrid solar integrated EV charging system. The hybrid system consists of a grid input to an LCL-filtered input connected to a single AC-DC power converter stage, followed by a dual active DC-AC-DC power converter stage, providing control and bidirectional power flow to the EV battery. The addition of a solar photovoltaic (PV) source between the two power conversion stages represents the primary innovation in this system. The PV source can be utilized as supplemental or as sole source of energy when there is no connection to the grid; thus allowing the charging system to operate continuously with no interruption. As opposed to the <math>Ga_2O_3</math>-based grid-only approach, the proposed system provides partial energy independence, encourages the utilization of renewable energy, and enhances the reliability of the overall system under varying grid conditions. This hybrid configuration is suitable for modern EV charging infrastructures</i></p>

## 1. INTRODUCTION

Highly effective, quick, and eco-friendly charging systems have been developed by means of innovative developments in the area of EV (electric vehicle) infrastructure. High rates of pollution and harm to human health are produced by the burning of fossil fuels used by conventional vehicles [1][2]. Electric Vehicles (EVs) or Battery Electric Vehicles (BEVs) will cut down on Greenhouse gas emissions, therefore lessening pollution and other negative effects caused by conventional vehicles [3][4]. Inadequate in regards to reliability, adaptability and ecological influence, conventional EV charging systems, generally depending upon the grid, are proving to be insufficient as a result of increased numbers of EVs [1]. Not only do these conventional systems put a lot of strain on the electrical grid during times of peak demand, but they are also limited in their ability to utilize renewable energy sources. Therefore, they cannot contribute to the development of de-carbonized transportation [11]. With an increase in the number of EVs, there is an increase in the amount of pressure on the central electrical grid, producing concerns over voltage fluctuation, peak load mismatch and overall decreased power quality, specifically when fast chargers are installed in groups [8].

To resolve the mentioned shortcomings, recent designs of EV charging systems are incorporating hybrid energy architectures that incorporate both grid supplies and renewable energy sources, such as solar photovoltaics (PV) [7][8]. The proposed EV charging system in this project combines solar integration with the EV charging process to enhance both available energy and operational reliability. The previously designed EV charging systems that were based on ultra-wide bandgap (UWBG) materials such as gallium oxide ( $\text{Ga}_2\text{O}_3$ ) for high frequency switching and fast DC charging, however relied solely on the grid for all their energy needs [9]. Although these  $\text{Ga}_2\text{O}_3$  based chargers have high efficiencies and reduced thermal loss, they are lacking in resilience due to their dependence on the grid. In contrast to previous designs, the new design of the EV charging system supports high speed charging while introducing decentralized renewable energy integration for continued operation and sustainability. The first stage of the system uses grid power passed through an

LCL (LC-LC) filter to reduce harmonic distortion and improve input power quality. The LCL filter eliminates high frequency switching noise, provides sinusoidal current flow and therefore complies with IEEE 519 standards for power quality [5][6]. The AC signal that is output from the LCL filter is then converted into a DC signal through an AC DC converter stage. The AC DC converter stage creates a stable DC link that is necessary for the subsequent processing. The AC DC converter also supports voltage regulation and current shaping to maintain a near unity power factor, which reduces the reactive power stress on the grid. The second stage of the system utilizes a Dual Active Bridge (DAB) DC AC DC converter, which supports bidirectional power flow, galvanic isolation, and efficient voltage regulation for the charging of EV batteries. The DAB topology is capable of supporting soft switching techniques such as Zero Voltage Switching and Zero Current Switching, which improves conversion efficiency at medium to high power levels [16][17]. The solar PV source is located between the AC DC and DAB stages and provides a hybrid energy path. The solar input is controlled by a Maximum Power Point Tracking (MPPT) controller that continuously adjusts the operating parameters of the solar array to optimize energy extraction based on irradiance and temperature conditions. Algorithms such as Perturb and Observe (P&O) or Incremental Conductance (IncCond) are commonly used as MPPT controllers to dynamically track the maximum power point [12][13]. This results in seamless continuation of the charging operation in the event of grid disconnection, which increases system reliability. The system architecture is also compatible with several modern energy flow concepts. The Grid to Vehicle (G2V) function allows the EV to be charged from the grid when it is in normal operation [14][15]. Future enhancements may include the incorporation of Vehicle to Grid (V2G) function, which would allow stored energy in the EV battery to be sent back to the grid during peak demand or emergency situations [10]. The Solar to Vehicle (S2V) function is supported through the integration of the PV, resulting in cleaner charging cycles. Additionally, in a microgrid or smart grid context, this architecture can be extended to support coordinated energy sharing between multiple vehicles and local renewable energy sources. The combination of the MPPT-controlled solar

input, two-stage conversion and advanced bidirectional power management enable the proposed system to provide an energy-efficient, reliable and ecologically

friendly solution for the next-generation EV charging infrastructure.

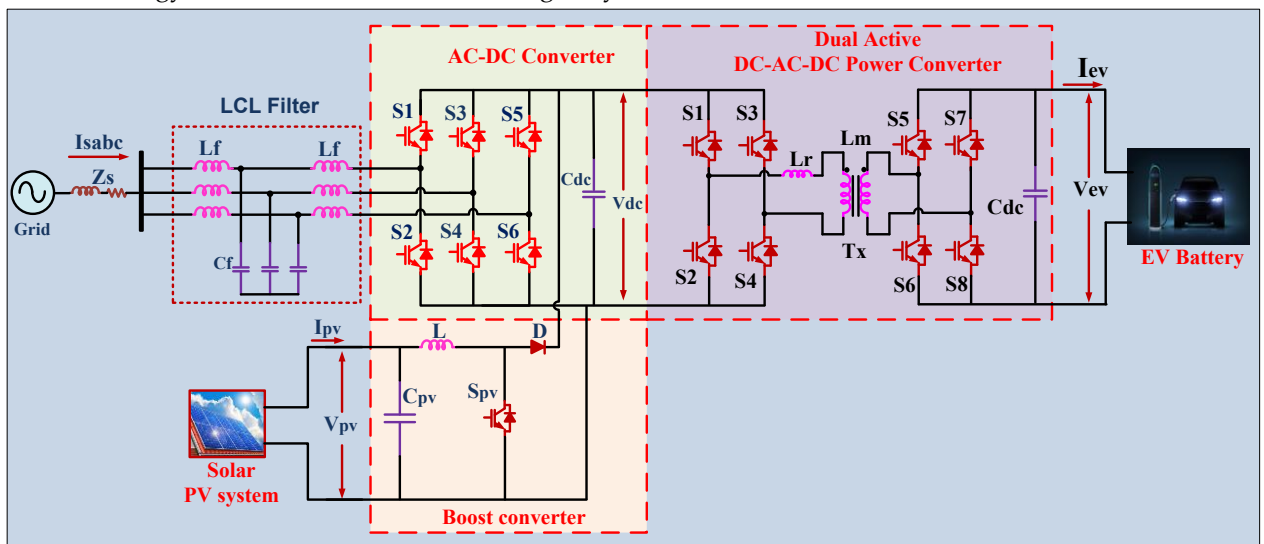


Fig.1 proposed system configuration

## 2. SYSTEM CONFIGURATION

The proposed electric vehicle (EV) charging system utilizes both grid power and solar energy to provide a constant source of energy to the vehicle during grid outages. As depicted in the figure, the grid is initially connected via a three-phase grid connection to an LCL filter. The LCL filter is comprised of inductors and capacitors that function to remove high frequency harmonic components and improve the overall quality of the current being supplied to the grid. The filtered AC power is then converted to DC via an AC-DC converter. The AC-DC converter includes six semiconductor devices and a DC-link capacitor as part of its design to minimize ripples and ensure a stable DC voltage. The stabilized DC voltage is required for the subsequent stages of power conversion and energy delivery to the EV. Following the AC-DC converter is the Dual Active DC-AC-DC Power Converter. The Dual Active DC-AC-DC Power Converter is comprised of two full-bridge converters with a high frequency transformer positioned between them. The first bridge is connected to the DC-link from the AC-DC converter while the second bridge is connected to the EV battery. The converter provides galvanic isolation and bidirectional power flow as well as efficiently delivers DC power to the battery. The converter controls the charging process by modulating the voltage and current in accordance with the needs of the EV battery. To further increase the

sustainability and reliability of the system, a solar photovoltaic (PV) system is incorporated between the AC-DC converter and the dual active bridge. The solar PV system is connected to the AC-DC converter via a boost converter. The boost converter boosts the voltage from the PV panels and supplies it to the common DC bus. The boost converter utilizes Maximum Power Point Tracking (MPPT) to dynamically regulate the operating point of the solar panel to maximize the amount of energy that can be extracted from the sun regardless of changing sunlight conditions. While the grid is operational, the majority of the energy will be supplied to the EV battery via the grid. If the grid is either disconnected or otherwise unavailable, the solar PV system will supply the energy to continue charging the EV battery. The hybrid configuration of this system provides the ability to maintain flexibility in charging options while minimizing the dependence upon the grid and supporting the use of renewable energy, ultimately providing an optimal solution for the development of sustainable EV infrastructure.

## 3. MODELING AND DESIGNING OF PROPOSED SYSTEM CONFIGURATION

### A. Solar PV system

The single diode model is capable of modeling the operation of a solar cell under different environmental factors, such as temperature and irradiation levels. When

light strikes the solar cell, the generated photocurrent  $I_{ph}$  will increase linearly with the irradiation level but will also have a slight dependence on temperature. the diode represents the p-n junction within the solar cell and will account for any recombination losses. the series resistance  $R_s$  will represent the internal resistance losses of the cell, while the shunt resistance  $R_{sh}$  will account for the leakages that may occur through the cell. the output current  $I$  will be determined by the difference between the photo-generated current and the diode leakage current minus any voltage drop across the series and shunt resistances. this equation is non-linear and typically needs to be solved iteratively for accurate simulation or design purposes. the operating voltage  $V$  can be varied to allow the solar cell to operate at different points along the I-V curve of the solar cell. at an open circuit condition, the current is equal to zero, and at a short circuit condition, the voltage is equal to zero. between the two extremes there exists a maximum power point (MPP) at which the product of the current and voltage (or power) is at its largest and represents the most efficient operating point of the pv cell. in practice, MPPT (maximum power point tracking) algorithms, such as incremental conductance or perturb and observe, are utilized in PV systems to dynamically vary the operating point of the PV system by either varying the load or the duty cycle of a DC-DC converter to remain as close to the MPP as possible under changing illumination conditions or temperatures. this allows for the greatest amount of energy to be extracted from the PV array. the single-diode model provides a commonly used and reliable framework for engineers to simulate and design PV systems to determine their expected performance under various conditions and to design system components such as dc-dc converters and energy storage.

#### a. Single Diode Model of a PV Cell

The single diode model is widely used to represent the electrical behavior of a solar cell or PV module, capturing its nonlinear current-voltage (I-V) characteristics.

1. Equivalent Circuit: A current source  $I_{ph}$  in parallel with a diode (with saturation current  $I_0$ ), series resistance  $R_s$ , and shunt resistance  $R_{sh}$ .

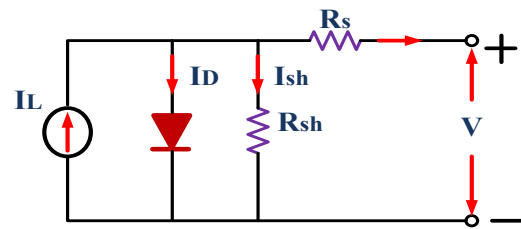


Fig. 2 equivalent model of PV solar.

#### 2. Output Current Equation:

$$I_{ph} - I_0 \left( e^{\frac{q(V+IR_s)}{nkT}} - 1 \right) - \frac{V+IR_s}{R_{sh}} \quad (1)$$

Where:

- $I$  = output current (A)
- $V$  = output voltage (V)
- $I_{ph}$  = photo-generated current (A)
- $I_0$  = diode saturation current (A)
- $q$  = electron charge  $1.602 \times 10^{-19}$  C
- $n$  = diode ideality factor (typically 1 to 2)
- $k$  = Boltzmann constant  $1.381 \times 10^{-23}$  J/K
- $T$  = cell temperature (Kelvin)
- $R_s$  = series resistance ( $\Omega$ )
- $R_{sh}$  = shunt resistance ( $\Omega$ )

#### 3. Photo-generated current $I_{ph}$ :

$$= [I_{sc} + K_i(T - T_{ref})] \times \frac{G}{G_{ref}} \quad (2)$$

Where:

- $I_{sc}$  = short-circuit current at reference temperature
- $K_i$  = temperature coefficient of current ( $A/^\circ C$ )
- $T_{ref}$  = reference temperature (usually  $25^\circ C$  or  $298$  K)
- $G$  = solar irradiance ( $W/m^2$ )
- $G_{ref}$  = reference irradiance ( $1000 W/m^2$ )

#### 4. Diode Saturation Current $I_0$ :

$$I_0 = I_{0_{ref}} \left( \frac{T}{T_{ref}} \right)^3 \exp \left( \frac{qE_g}{nk} \left( \frac{1}{T_{ref}} - \frac{1}{T} \right) \right) \quad (3)$$

Where:

- $I_{0_{ref}}$  = diode saturation current at  $T_{ref}$
- $E_g$  = bandgap energy of the semiconductor (eV)

#### 5. Open-circuit voltage $V_{oc}$ :

$$V_{oc} = \frac{nkt}{q} \ln \left( \frac{I_{ph}}{I_0} + 1 \right) \quad (4)$$

## B. Solar PV boost Converter

The Boost Converter is a DC-DC converter that increases the Input Voltage to a higher Output Voltage as shown in FIG. 3. The main components are an inductor (L), A Switch (Normally a MOSFET), A Diode (D), and An Output Capacitor (C). When the MOSFET is ON, the MOSFET closes, and Current can Flow from the Photovoltaic (PV) Panel Through the Inductor and Store Energy in the Magnetic Field of the Inductor While the Diode is Reverse Biased, thus Preventing Current From Reaching the Output. When the MOSFET Turns OFF, the MOSFET Opens, and the Magnetic Field Collapses and Releases the Stored Energy. The Inductor's Current then Flows Through the Diode to the Output Capacitor and Load, Effectively Adding to the Input Voltage, Resulting in a Higher Output Voltage Than the Input Voltage. This Process Allows for Efficient Voltage Boosting Suitable For Charging Batteries Or Powering Loads.

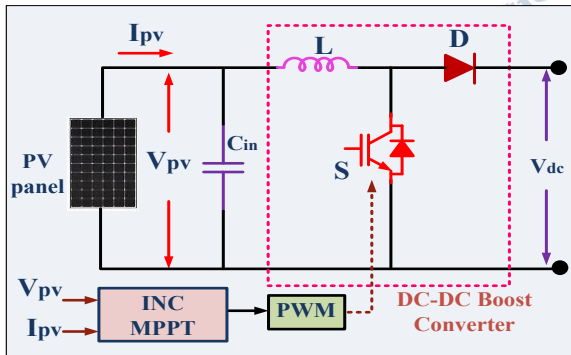


Fig. 3 solar PV INC MPPT DC-DC boost converter

### 1. Output Voltage of Boost Converter

$$V_o = \frac{V_{in}}{1-D} \quad (5)$$

Where:  $V_o$ : Output voltage,  $V_{in}$ : PV input voltage,  $D$ : Duty cycle ( $0 < D < 1$ )

### 2. Inductor Value (L)

$$L = \frac{V_{in} \cdot D}{f_s \cdot \Delta I_L} \quad (6)$$

Where:

- $f_s$ : Switching frequency (Hz)
- $\Delta I_L$ : Inductor ripple current (A), usually 20–40% of  $I_{in}$

### 3. Output Capacitor Value (C)

$$C = \frac{I_o \cdot D}{f_s \cdot \Delta V_o} \quad (7)$$

Where:

- $I_o$ : Output current (A)

- $\Delta V_o$ : Acceptable output voltage ripple (V)

## C. MPPT Control

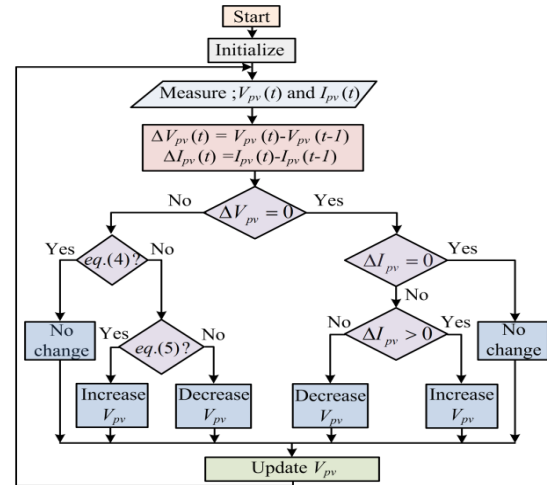


Fig. 4. INC MPPT control

Fig. 4 depicts the solar PV array's greatest power point technique. It generates a voltage reference ( $V^*_{pv}$ ) that is the same as the MPP voltage of the PV array.

At the MPP,

$$\frac{dP_{PV}}{dV_{PV}} = 0 \quad (8)$$

$$\frac{d(V_{PV} I_{PV})}{dV_{PV}} = I_{PV} + V_{PV} \frac{dI_{PV}}{dV_{PV}} = 0 \quad (9)$$

$$\frac{dI_{PV}}{dV_{PV}} = -\frac{I_{PV}}{V_{PV}} \quad (10)$$

Right side displays PV array instantaneous conductance.

Conditions of INC MPPT control:

$$\frac{dI_{PV}}{dV_{PV}} = -\frac{I_{PV}}{V_{PV}} \left( \frac{dP_{PV}}{dV_{PV}} = 0, \text{ at MPP} \right) \quad (11)$$

$$\frac{dI_{PV}}{dV_{PV}} > -\frac{I_{PV}}{V_{PV}} \left( \frac{dP_{PV}}{dV_{PV}} > 0, \text{ at left of MPP} \right) \quad (12)$$

$$\frac{dI_{PV}}{dV_{PV}} < -\frac{I_{PV}}{V_{PV}} \left( \frac{dP_{PV}}{dV_{PV}} < 0, \text{ at right of MPP} \right) \quad (13)$$

According to the circumstances, the disturbance arises in the PV array's voltage, which is used to monitor the array's maximum power point.

## 4. DESIGN OF WPT DUAL ACTIVE BRIDGE CONVERTER

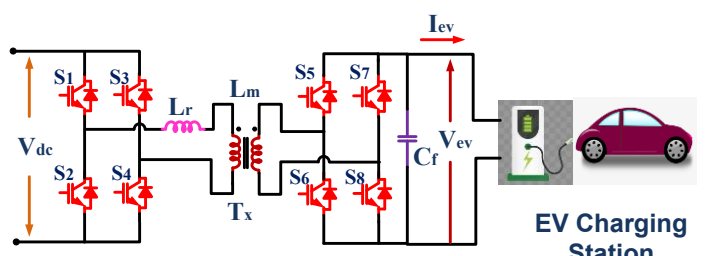


Fig.5 Designing of wireless dual active bridge converter for EV charging

The WPT-DAB converter is a high-frequency bidirectional DC-DC converter that is specifically designed to efficiently transfer electrical energy from a DC source to a load in Electric Vehicle (EV) Fast Charging Applications. This type of converter has two Active Full-Bridge (AFB) Circuits, a High Frequency Transformer (HFT), and a Resonant Circuit. Together these elements allow the converter to operate in Soft-Switching mode which minimizes Losses. The converter operates at high Switching Frequencies (typically 85 kHz to 150 kHz). These high Switching Frequencies enable the use of smaller transformers and yet maintain a high level of Efficiency. In order to transfer the high frequency Alternating Current (AC) generated by each of the primary and secondary AFBs through the HFT and subsequently convert the transferred AC back into DC at the Output, the resonant tank circuit (consisting of Inductor L<sub>r</sub> and Capacitor C<sub>r</sub>) allows for Soft-Switching Operation. This reduced Stress on the Power Semiconductors.

In designing the WPT-DAB converter, the first step in the Design Process is to select the Appropriate Turns Ratio (n) of the Transformer, next is to Optimize the Switching Frequency (f<sub>s</sub>), and lastly to determine the Required Values of the Resonant Inductor (L<sub>r</sub>) and Capacitor (C<sub>r</sub>) to Ensure Reliable and Stable Power Transfer. The DC Link Voltage is Regulated using a Frequency Control Algorithm, Whereby any Deviations from the Resonant Frequency are Monitored and Used as Input to Dynamically Adjust the Operating Frequency, Enhancing Overall Efficiency. The Controller Utilizes Phase Shift Modulation (PSM) to Regulate Power Flow by Adjusting the Phase Difference ( $\phi$ )

Between the Primary and Secondary Bridges. The Operating Frequency of the WPT-DAB converter can be Reduced when the SOC of the EV Battery is Low, thereby Reducing the Input Voltage and Maintaining Efficient Charging Conditions. Furthermore, the converter will avoid Series Resonance During High-Voltage AC Mains Variations, Ensuring Reliable Performance. The Mathematical Formulation of the WPT-DAB Converter is Based on Power Transfer and Soft-Switching Conditions. The Transferred Power (P) in Terms of Phase Shift ( $\phi$ ) and Resonant Parameters is Given by:

$$P = \frac{V_1 V_2}{n L_r f_s} \phi (1 - \phi) \quad (14)$$

where V<sub>1</sub> and V<sub>2</sub> are the primary and secondary voltages, n is the transformer turns ratio, L<sub>r</sub> is the resonant inductor, and f<sub>s</sub> is the switching frequency. The resonant frequency is given by:

$$f_r = \frac{1}{2\pi\sqrt{L_r C_r}} \quad (15)$$

ensuring that the system operates in the optimal soft-switching region. The phase shift ( $\phi$ ) control is essential for adjusting power flow dynamically, maintaining efficient energy transfer. The zero-voltage switching (ZVS) condition is achieved when:

$$\phi \geq \frac{L_r I_0}{V_1} \quad (16)$$

where I<sub>0</sub> is the output current. By implementing these control strategies, the WPT-DAB converter significantly improves power transfer efficiency, reduces switching losses, and ensures fast and flexible EV charging with minimal stress on power components.

## 5. CONTROL ALGORITHM

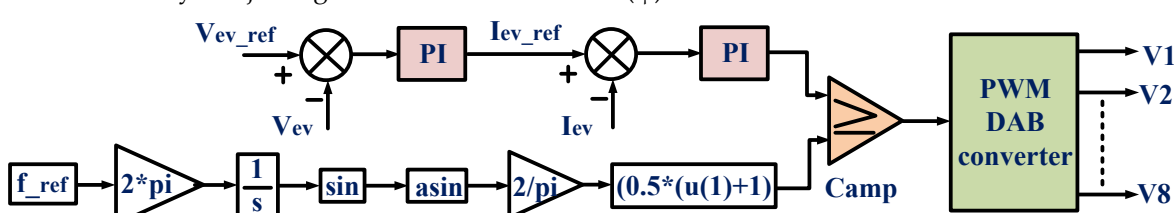


Fig.4 controller design for dual active bridge converter for fast electric vehicle charging station

1. Power Flow from Primary to Secondary (Charging Mode):
  - Occurs when the primary voltage leads the secondary voltage (positive phase shift).
  - Energy flows from DC source/grid to battery.
2. Power Flow from Secondary to Primary (Discharging Mode):
  - Occurs when the secondary voltage leads the primary voltage (negative phase shift).
  - Energy flows from battery to DC grid or loads.

This phase-shift control enables bidirectional power transfer with high efficiency, fast response, and soft-switching (ZVS).

#### a. Power Transfer Equation:

The average power transferred from primary to secondary is:

$$P = \frac{nV_1V_2}{\omega L} \cdot \phi \cdot \left(1 - \frac{|\phi|}{\pi}\right) \text{ (for small } \phi\text{)} \quad (17)$$

Where:

- $\omega = 2\pi f_s$
- $\phi \in [-\pi, \pi]$

## 6. DC-LINK VOLTAGE CONTROLLER DESIGN

The DC-link voltage ( $V_{dc}$ ) is regulated using a PI controller to ensure stable operation during bidirectional power transfer. The power balance at the DC bus is given by:

$$C_{dc} \frac{dV_{dc}}{dt} = \frac{3}{2} (V_d I_d + V_q I_q) - P_{dc\_load} \quad (21)$$

where:  $C_{dc}$  = DC-link capacitor,  $P_{dc\_load}$  = Power consumed by the DC load

To maintain a stable DC-link voltage, a PI controller is implemented as:

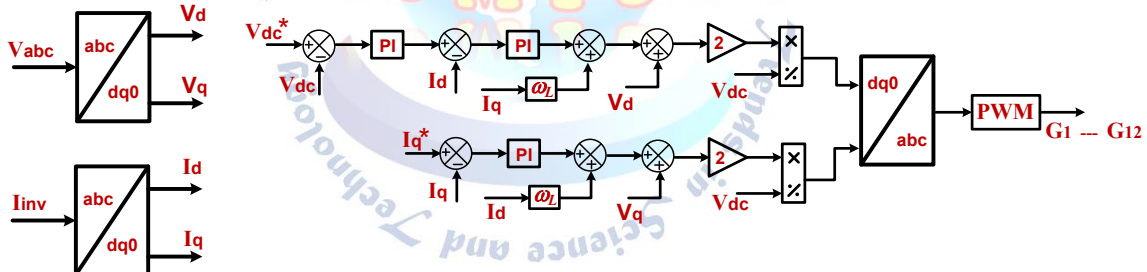


Fig. 8 Grid conversion controller

## 7. RESULTS AND DISCUSSION

The solar-assisted electric vehicle charging system was evaluated under different operating conditions using simulations to verify that the proposed system works properly both when connected to and disconnected from the electrical grid. In the case of the electrical grid being available and operational, the LCL (Leakage Inductance Clamp) filter reduced the level of distortion caused by harmonics; the AC-DC converter produced a stable DC output voltage at the DC link that served as an input to the dual-active DC-AC-DC power converter. The dual active converter regulated the charging voltage and current to the EV battery and allowed for bidirectional flow of power between the source and the load while

$$I_d^{ref} = K_p (V_{dc}^{ref} - V_{dc}) + k_i \int (V_{dc}^{ref} - V_{dc}) dt \quad (22)$$

Where:  $K_p, K_i$  = Proportional and integral gains of the PI controller,  $I_d^{ref}$  = Reference d-axis current

#### a. d-q Current Controller Design

The d-axis and q-axis current controllers regulate the power exchange between the converter and the grid.

#### b. d-Axis Current Controller (Active Power Control)

The d-axis current controller regulates the active power ( $P$ ) supplied to or drawn from the grid. The reference current is obtained from the DC-link voltage controller:

$$I_d^{ref} = \frac{P^{ref}}{1.5V_d} \quad (23)$$

Using a PI compensator, the d-axis voltage command is:

$$V_d^{ref} = K_p^d (I_d^{ref} - I_d) + K_i^d \int (I_d^{ref} - I_d) dt \quad (24)$$

Where  $K_p^d, K_i^d$  are PI gains

#### c. q-Axis Current Controller (Reactive Power Control)

The q-axis current controller regulates reactive power ( $Q$ ), and the reference current is:

$$I_q^{ref} = \frac{Q^{ref}}{1.5V_q} \quad (25)$$

The q-axis voltage command is:

$$V_q^{ref} = K_p^q (I_q^{ref} - I_q) + K_i^q \int (I_q^{ref} - I_q) dt \quad (26)$$

providing soft-switching operation and a smooth and predictable charging pattern. Output voltage  $V_{ev}$  and current  $I_{ev}$  were shown to fall within the established limits for the chosen EV battery; this ensured safe operation and reliability. Additionally, the dual-active converter provided galvanic isolation due to the presence of a high frequency transformer and continued to provide a constant output regardless of transient changes in the grid. When the electrical grid was disconnected, the solar photovoltaic (PV) system, coupled with a boost converter, provided the necessary power to continue charging the battery. A maximum power point tracking (MPPT) controller was implemented into the boost converter; this allowed the

duty cycle of the boost converter to dynamically adjust to optimize the amount of power extracted from the PV panels under variable irradiance conditions. The simulation demonstrated that even though the solar irradiance varied, the MPPT-controlled boost converter maintained a stable DC-link voltage and allowed the dual-active converter to operate uninterrupted. The comparison demonstrates that the proposed charging system is able to charge continuously without the need for an external back-up or interruption; this is contrary to traditional grid-based charging systems. Not only does the use of solar input reduce the strain on the grid, but it promotes the consumption of green energy. In addition, the dual-converter topology allows for higher efficiency in the conversion of power, improved power quality and provides for potential expansion into Vehicle-to-Grid (V2G) or other smart grid applications. Overall, the results demonstrate the ability of the system to provide reliable and efficient operation under both solar and grid conditions. The overall performance of the proposed system in regards to power quality, energy continuity and renewable energy integration makes it well-suited for the development of advanced EV charging infrastructure.

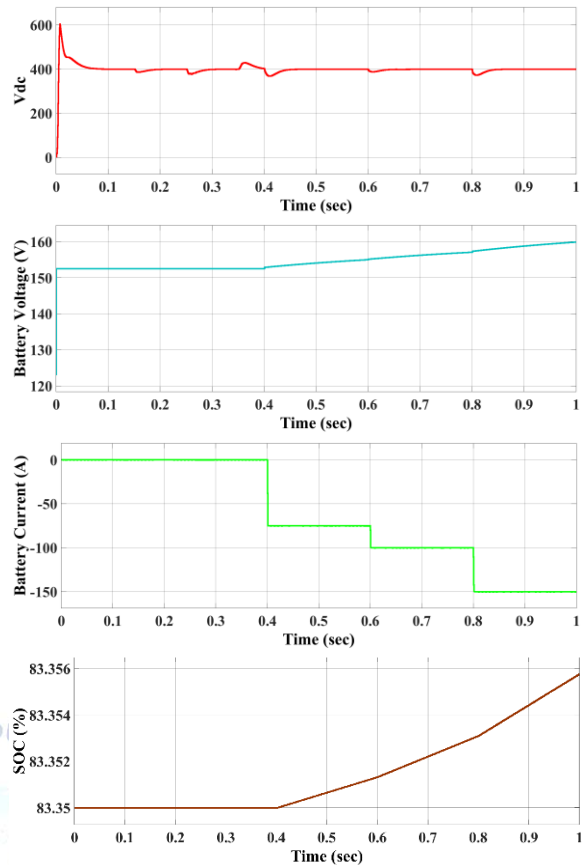
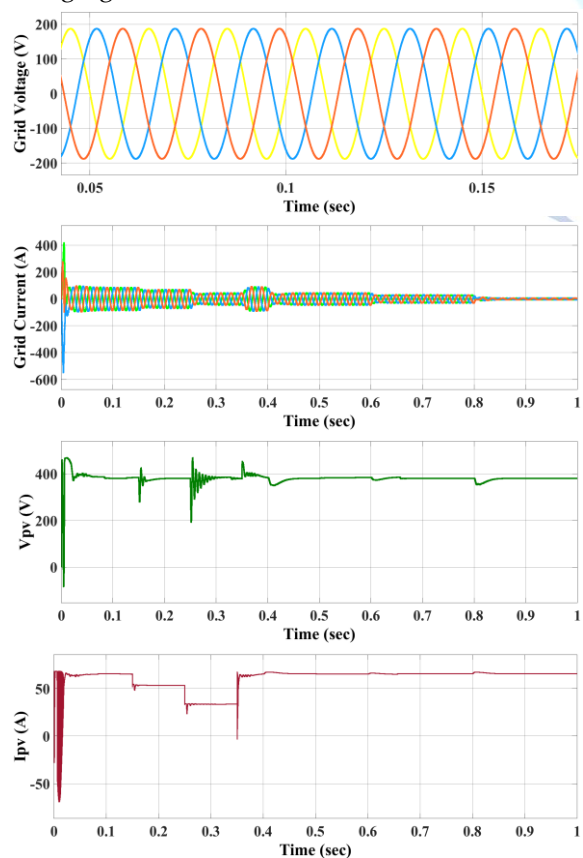


Fig.6 Simulation results of the Hybrid Solar-Battery Bidirectional Wireless Power Transfer System for EV Charging under Variable Irradiance Conditions

## 8. CONCLUSION

This project is a successful hybrid electric vehicle (EV) charging system that combines the use of grid power and solar energy for charging. The hybrid EV charger utilizes an LCL filter to enhance the power quality; an AC-DC converter for rectification; and a Dual Active DC-AC-DC Converter to ensure high-efficiency and isolated power transfer from the grid/solar panel to the EV's battery. A solar PV system integrated with maximum power point tracking (MPPT) is used to ensure continuous EV charging during grid outages, and promote the use of renewable energy. Simulations demonstrate that the hybrid EV charging system will operate continuously in all scenarios as indicated by stable voltages/currents in each scenario. The proposed EV charger design offers improved energy efficiency compared to traditional charging systems; provides support to the adoption of green energy solutions; and can provide continuous EV charging, which represents a viable solution for the creation of future EV charging stations.

## Conflict of interest statement

Authors declare that they do not have any conflict of interest.

## REFERENCES

[1] S. Habib, M. M. Khan, F. Abbas, A. Ali, M. T. Faiz, F. Ehsan, and H. Tang, "Contemporary trends in power electronics converters for charging solutions of electric vehicles," *CSEE J. Power Energy Syst.*, vol. 6, no. 4, pp. 911–929, Dec. 2020, doi: 10.17775/CSEEJPES.2019.02700.

[2] M. R. Khalid, I. A. Khan, S. Hameed, M. S. J. Asghar, and J.-S. Ro, "A comprehensive review on structural topologies, power levels, energy storage systems, and standards for electric vehicle charging stations and their impacts on grid," *IEEE Access*, vol. 9, pp. 128069–128094, 2021, doi: 10.1109/ACCESS.2021.3112189.

[3] S. Chakraborty, H.-N. Vu, M. M. Hasan, D.-D. Tran, M. E. Baghdadi, and O. Hegazy, "DC-DC converter topologies for electric vehicles, plug-in hybrid electric vehicles and fast charging stations: State of the art and future trends," *Energies*, vol. 12, no. 8, p. 1569, Apr. 2019, doi: 10.3390/en12081569.

[4] T. Gnann, S. Funke, N. Jakobsson, P. Plötz, F. Sprei, and A. Bennehag, "Fast charging infrastructure for electric vehicles: Today's situation and future needs," *Transp. Res. D, Transp. Environ.*, vol. 62, pp. 314–329, Jul. 2018, doi: 10.1016/j.trd.2018.03.004.

[5] Limits for Harmonics Current Emissions (Equipment Current 16A Per Phase), IEC Standard IEC 61000-3-2, 2000.

[6] IEEE Standard for Harmonic Control in Electric Power Systems, IEEE Standard 519-2022 (Revision of IEEE Standard 519-2014), Aug. 2022.

[7] Y. Jeong, J. K. Kim, and G. W. Moon, "A bridgeless dual boost rectifier with soft switching capability and minimized additional conduction loss," *IEEE Trans. Ind. Electron.*, vol. 65, no. 3, pp. 2226–2233, Mar. 2018.

[8] A. Malschitzky, F. Albuquerque, E. Agostini, and B. N. Claudinor, "Single-stage integrated bridgeless-boost nonresonant half-bridge converter for LED driver applications," *IEEE Trans. Ind. Electron.*, vol. 65, no. 5, pp. 3866–3878, May 2018.

[9] L. Sun, C. Yang, and H. M. Nguyen, "Uncoordinated EV charging impact on power distribution networks: A case study," *Applied Energy*, vol. 322, 2023.

[10] A. S. Jadhav and K. P. Bhattacharya, "Demand-side management strategies for mitigating peak loads in EV-integrated grids," *Energy Reports*, vol. 8, pp. 1875–1889, 2022.

[11] Z. Lin, L. Zhang, and M. Sun, "Wireless EV charging: A review of recent advancements," *IEEE Transactions on Transportation Electrification*, vol. 9, no. 1, 2023.

[12] K. Divya and J. Østergaard, "Battery energy storage technology for power systems—An overview," *Electric Power Systems Research*, vol. 79, no. 4, pp. 511–520, Apr. 2009.

[13] X. Luo, J. Wang, M. Dooner, and J. Clarke, "Overview of current development in electrical energy storage technologies and the application potential in power system operation," *Applied Energy*, vol. 137, pp. 511–536, Jan. 2015.

[14] A. S. Alsharif, A. M. Shalaby, M. A. Badawy, and H. M. Ismail, "Optimal energy management system for grid-connected hybrid renewable power system in EV charging station," *Sustainable Energy Technologies and Assessments*, vol. 43, p. 100957, 2021.

[15] C. Liu, K. T. Chau, and X. Zhang, "An efficient wind-photovoltaic hybrid generation system using doubly excited permanent-magnet brushless machine," *IEEE Trans. Industrial Electronics*, vol. 57, no. 3, pp. 831–839, Mar.